

High power and spectral purity continuous-wave photonic THz source tunable from 1 to 4.5 THz for nonlinear molecular spectroscopy

J Kiessling^{1,5}, I Breunig², P G Schunemann³, K Buse^{1,2}
and K L Vodopyanov⁴

¹ Fraunhofer Institute of Physical Measurement Techniques, Heidenhofstraße 8, D-79110 Freiburg, Germany

² Laboratory for Optical Systems, Department of Microsystems Engineering—IMTEK, University of Freiburg, Georges-Köhler-Allee 102, D-79110 Freiburg, Germany

³ BAE Systems Inc., Nashua, NH 03061, USA

⁴ CREOL, College of Optics & Photonics, University of Central Florida, Orlando, FL 32816, USA

E-mail: jens.kiessling@ipm.fraunhofer.de

New Journal of Physics **15** (2013) 105014 (11pp)

Received 24 June 2013

Published 18 October 2013

Online at <http://www.njp.org/>

doi:10.1088/1367-2630/15/10/105014

Abstract. We report a diffraction-limited photonic terahertz (THz) source with linewidth < 10 MHz that can be used for nonlinear THz studies in the continuous wave (CW) regime with uninterrupted tunability in a broad range of THz frequencies. THz output is produced in orientation-patterned (OP) gallium arsenide (GaAs) via intracavity frequency mixing between the two closely spaced resonating signal and idler waves of an optical parametric oscillator (OPO) operating near $\lambda = 2 \mu\text{m}$. The doubly resonant type II OPO is based on a periodically poled lithium niobate (PPLN) pumped by a single-frequency Yb:YAG disc laser at 1030 nm. We take advantage of the enhancement of both optical fields inside a high-finesse OPO cavity: with 10 W of 1030 nm pump, 100 W of intracavity power near $2 \mu\text{m}$ was attained with GaAs inside cavity.

⁵ Author to whom any correspondence should be addressed.



Content from this work may be used under the terms of the [Creative Commons Attribution 3.0 licence](http://creativecommons.org/licenses/by/3.0/).

Any further distribution of this work must maintain attribution to the author(s) and the title of the work, journal citation and DOI.

This allows dramatic improvement in terms of generated THz power, as compared to the state-of-the art CW methods. We achieved $>25 \mu\text{W}$ of single-frequency tunable CW THz output power scalable to $>1 \text{ mW}$ with proper choice of pump laser wavelength.

Contents

| | |
|--|-----------|
| 1. Introduction | 2 |
| 2. Photonic terahertz (THz) generation with resonant enhancement of two optical waves inside an optical parametric oscillator (OPO) | 3 |
| 3. Experimental setup | 4 |
| 4. Orientation-patterned GaAs samples | 5 |
| 5. OPO operation | 5 |
| 6. Generation of THz waves | 6 |
| 7. THz linewidth | 9 |
| 8. Potential for continuous single-frequency THz tuning | 10 |
| 9. Conclusion | 10 |
| Acknowledgments | 11 |
| References | 11 |

1. Introduction

Photonic generators of THz waves based on optical rectification, photoconductive antennae and photomixers, three-wave mixing processes in crystals and four-wave processes in air plasma—all acquired great popularity in the last two decades, not to the least extent because of the variety of coherent photonic sources available on the market that operate in the continuous wave (CW), nano-, pico- and femtosecond regimes [1, 2]. The major attractiveness of lasers as driving sources for terahertz (THz) devices comes from their compactness, high wall-plug efficiency (especially for diode-pumped solid state and fiber lasers) and ability to work at room temperature. A major progress has been observed in the femtosecond domain, where $>10^{-3}$ optical-to-THz conversion efficiencies are routinely attainable, and THz pulse intensities as high as 10 MW cm^{-2} are achieved [3]. Clearly, these sources are well suited for nonlinear THz studies of condensed matter, e.g. semiconductors, solids and liquids. Low-density molecular gases on the other hand, experience very sharp resonances in the THz domain, associated with their high- Q rotational modes and as a result high-resolution THz spectroscopy has enormous potential for the chemical analysis of gases. Typically, the linewidths are pressure broadened, but at low pressures ($<10 \text{ m torr}$) the Doppler broadening dominates leading to the linewidths of $\sim 1 \text{ MHz}$.

Saturation (Lamb-dip) THz spectroscopy [4] applied to rotational bands in low-density molecular gases allows to reveal the fine structure hidden under the Doppler contour. However one needs sufficient THz power, high spectral purity and good beam quality to saturate molecular transitions. Winnewisser *et al* [5] used tunable narrow-linewidth ($<20 \text{ kHz}$) backward-wave oscillator (BWO) to perform sub-Doppler saturation-dip spectroscopy of rotational transitions of CO to reveal the upper limit for the Doppler—free linewidths of

16 kHz at 230 GHz, 25 kHz at 461 GHz and 32 kHz at 691 GHz. For the rotational transition of CO molecule at 1.15 THz, assuming homogeneously broadened full-width at half-maximum linewidth of $\Delta\nu_{\text{hom}} \sim 30$ kHz, one can estimate, based on the known line strength for this transition, $S = 1.3 \times 10^{-21} \text{ cm mol}^{-1}$ ⁶, the peak absorption cross section $\sigma = 2S/(\pi \Delta\nu_{\text{hom}}) = 8.3 \times 10^{-16} \text{ cm}^{-2}$ and saturation intensity $I_s = h\nu/(2\sigma\tau) = 1.4 \times 10^{-2} \text{ W cm}^{-2}$, where τ is the upper state lifetime $\sim 1/\Delta\nu_{\text{hom}}$. For a 1 m long gas cell and confocal focusing at 1.15 THz (beamsize $w \approx 0.64$ cm), we estimate the saturating power of $P_s \approx 10$ mW. This estimate assumes that the THz beam is diffraction limited and has narrow linewidth (< 30 kHz). Thus, in order to observe a 1% saturation dip in the spectrum, one needs at least $100 \mu\text{W}$ of THz power.

At frequencies above 1 THz, the power of BWO declines sharply and its use in the nonlinear spectroscopy is problematic [1]. Photomixers based on low-temperature-grown GaAs can generate narrow-bandwidth output in the whole THz range [6, 7], and THz linewidth is derived from that of near-IR pump lasers that can be as narrow as 10 kHz. However at > 0.3 THz the power rolls off as the fourth power of the frequency, due to finite lifetime of generated electron-hole pairs and parasitic capacitance of the emitter: the reported output power falls from $1 \mu\text{W}$ at 1 THz to about 1 nW at 3 THz [6]. Using $\chi^{(2)}$ process, CW narrow-bandwidth THz output with spectral width ~ 2 MHz was produced via difference frequency generation in a LiNbO₃ waveguide using two 760 mW CW lasers operating near $\lambda = 1.5 \mu\text{m}$ [8]. The output average power was 75 nW (tunable from 1.3 to 1.4 THz), which is clearly small for nonlinear studies.

Narrow-linewidth (~ 1 MHz) CW THz output tunable between 1.3 and 1.7 THz was produced in a cascaded parametric process, where the resonantly enhanced near infrared ‘signal’ wave of a primary 1030 nm pumped PPLN OPO served as pump for the secondary OPO (utilizing the same PPLN crystal and the same optical cavity) with the backward THz wave as the ‘idler’ [9]. In another setup based on a pump enhancement cavity with a finesse of 500 at the 1030 nm pump wavelength, the pump radiation was directly converted to the THz, via OPO process using PPLN, with the tunability from 1.2 to 2.9 THz [10]. In both cases the output power was limited to few μW due to strong THz absorption in lithium niobate.

A high-power CW THz source emitting up to 2 mW of THz power was reported, based on intracavity difference frequency generation in slanted PPLN that was placed inside the cavity of a dual-color vertical external cavity surface emitting laser [11]. THz output at two selected frequencies of 1 and 1.9 THz was reported and no data on THz linewidth was available.

Here we describe a high-power and high spectral purity THz source based on GaAs nonlinear crystal, which is able to cover continuously the whole 1–4.5 THz range and is suitable for nonlinear THz studies with low-density molecular gases.

2. Photonic terahertz (THz) generation with resonant enhancement of two optical waves inside an optical parametric oscillator (OPO)

Intracavity THz generation using a doubly resonant optical parametric oscillator (DR-OPO) was first proposed and implemented in [12], where a quasi-phase-matched (QPM) OP-GaAs crystal was placed inside the cavity of an OPO that was synchronously pumped by 7 ps 1064 nm pulses at 50 MHz repetition rate. The OPO was designed for type II parametric interaction

⁶ HITRAN database; <http://www.cfa.harvard.edu/HITRAN/>.

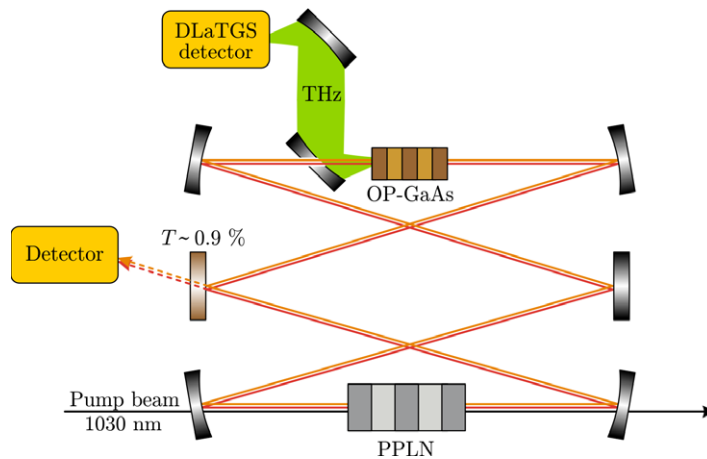


Figure 1. DR-OPO based on a PPLN pumped at 1030 nm with an additional OP-GaAs crystal for intracavity difference frequency generation.

(signal and idler orthogonally polarized) to allow narrow linewidths when operating near degeneracy. In the DR-OPO, both the signal and the idler waves resonate and the output THz power scales as cavity finesse squared. Despite of high loss in the cavity $\sim 20\%$, 1 mW of average power was generated at 2.8 THz (bandwidth 300 GHz) in a diffraction-limited beam [12].

The main innovation of this work is that the OPO operates CW and thus allows getting narrow linewidths. Also, in contrast to [12], we utilize advanced low-loss OP-GaAs structures and use a ring cavity that has smaller roundtrip loss and is more resistant to induced thermal lensing.

3. Experimental setup

A DR-OPO (figure 1) is pumped by a single-frequency (linewidth < 1 MHz) Yb:YAG disc laser operating at 1030 nm with maximum power of 17 W. A ring type 73.5 cm long OPO cavity is formed by six mirrors: two pairs of concave mirrors with radius of curvature 100 mm and two flat folding mirrors. All mirrors are highly transmissive ($> 99\%$) at the pump wavelength and highly reflecting ($> 99.9\%$) around 2060 nm, the OPO degeneracy wavelength, except for the outcoupler mirror transmitting $0.9 \pm 0.1\%$ for intracavity power monitoring. A 2.5 cm long periodically poled lithium niobate (PPLN) crystal, serving as the OPO gain element, is placed in one focal point of the resonator (beam waist, $1/e^2$ intensity radius, $w = 77 \mu\text{m}$). With the $13.5 \mu\text{m}$ domain reversal period of PPLN, we achieve type II quasi-phase matching with signal and idler waves close to degeneracy with crossed polarizations. These two waves are mixed in the OP-GaAs crystal placed in the second focal point of the cavity (beam waist $w = 90 \mu\text{m}$) to produce THz output. To extract the THz wave from the cavity, we use a 90° off-axis parabolic mirror with a 1 mm diameter hole transmitting the resonating optical waves. We measured the power of the generated THz wave using a calibrated DLaTGS pyroelectric detector (Bruker Optics) with black polyethylene filters used to block the near-IR. The total (signal + idler) intracavity power was determined by measuring the power of the $2 \mu\text{m}$ light transmitted through the outcoupling $T = 0.9\%$ mirror.

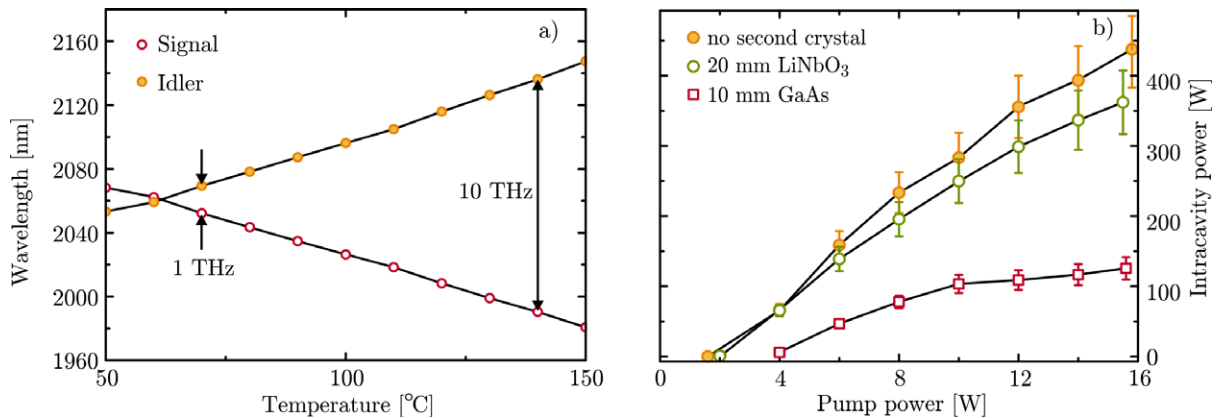


Figure 2. (a) OPO temperature tuning curves and (b) intracavity power versus pump power dependence. Solid lines are guides to the eye.

4. Orientation-patterned GaAs samples

Orientation-patterned GaAs crystals were grown at BAE systems by a combination of molecular beam epitaxy and hydride vapor phase epitaxy [13]. The samples were 5 and 10 mm long with useful aperture of 0.8 mm (height) by 5 mm (width), with three different QPM periods of $\Lambda = 1700, 780$ and $460 \mu\text{m}$, nominally designed for producing THz waves correspondingly around 1, 2 and 3 THz. The samples were antireflection coated for the center wavelength near $2.1 \mu\text{m}$ and were thermally contacted to an aluminum holder whose temperature was stabilized at 15°C using a Peltier cooler.

5. OPO operation

The DR-OPO is interferometrically sensitive to the cavity length [12]. Therefore, a piezoelectric actuator was attached to one of the mirrors and the OPO performance was optimized by slowly ramping the piezo voltage in one direction. Firstly, we measured the OPO temperature tuning curves. One can see (figure 2(a)) that by varying the temperature of the PPLN crystal from 60 to 100°C the difference frequency of the signal and idler waves can be changed in a big range, from 0.2 to 10 THz.

Secondly, we determined the total intracavity power of the signal and idler waves as a function of the input power at 1030 nm wavelength. The results for different OPO configurations are displayed in figure 2(b). For each configuration, the beam waists in the two focal spots of the resonator were kept constant. If there is no DFG crystal in the cavity, the oscillation threshold is $P_{\text{th}} \approx 1.6 \text{ W}$ and the total intracavity power grows up to $P_{\text{ic}} = 440 \text{ W}$ at $P_{\text{pu}} = 15.6 \text{ W}$. Inserting a 20 mm long lithium niobate crystal as passive element in the second waist of the cavity increases the oscillation threshold to $P_{\text{th}} = 2 \text{ W}$ and decreases the maximum intracavity power by 20%. Most likely, this is caused by extra roundtrip loss due to imperfect antireflection coating of this crystal. The situation changes significantly if GaAs is placed inside the resonator. A 10 mm long OP-GaAs increases the pump threshold to 4 W and limits the highest intracavity power to 120 W. Furthermore, the measured pump depletion drops from 53% (20 mm long LiNbO₃) to 27% (10 mm long GaAs). This behavior cannot be explained exclusively by residual surface reflections of GaAs estimated to be $< 1\%$.

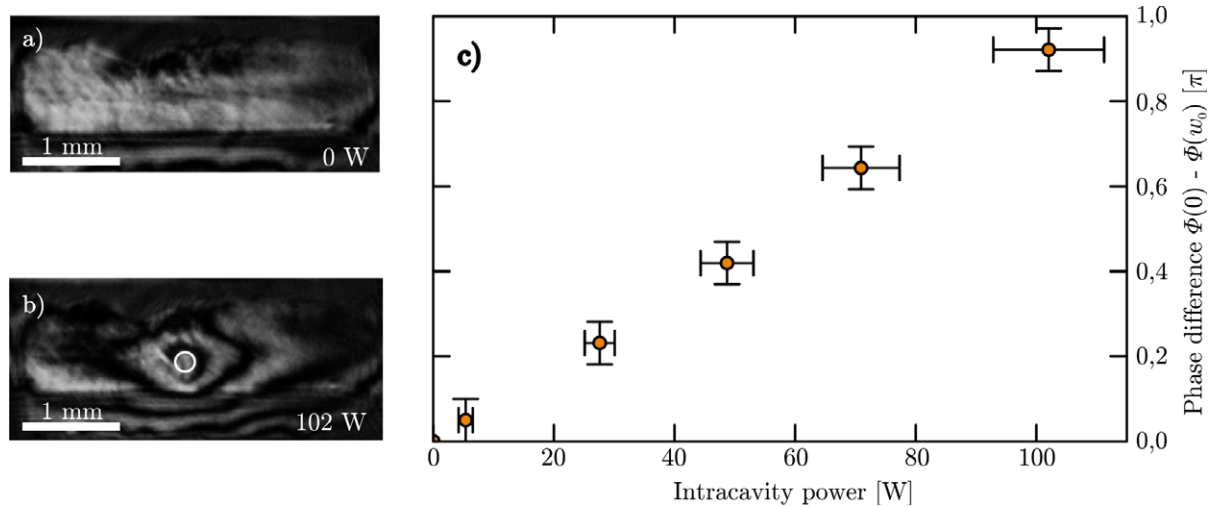


Figure 3. Mach–Zender interferograms of the 10 mm long OP-GaAs inside the OPO cavity indicating light-induced phase shifts. (a) Below the OPO oscillation threshold and (b) above threshold at 102 W intracavity power. (c) Thermally induced phase shift between the beam center and at beam radius w_0 versus intracavity power.

In order to investigate the drop in circulating power, we have set up, around GaAs, a Mach–Zender interferometer operating at 1030 nm that enables to determine phase shifts induced by the intracavity light field during the OPO operation. At pump power < 4 W, that is below the oscillation threshold with no circulating $2 \mu\text{m}$ waves, we do not observe any light induced phase shifts (figure 3(a)). However, at $P_{\text{ic}} = 102$ W (figure 3(b)) one can clearly see that the $2 \mu\text{m}$ radiation generates a lens into the GaAs crystal. The strength of the lens increases monotonously with the intracavity power (figure 3(c)). From figure 3(b) we estimated that at 102 W intracavity power, the induced lens has an equivalent focal length of $f \approx 25$ mm (in a thin-lens approximation). At this power the phase difference induced between the beam center and a distance of w_0 away from the beam center is approximately π (see figure 3(c)) which reduces the power coupling of the thermally aberrated beam to a Gaussian TEM_{00} mode to below 30% [15]. Thus we conclude that a thermal lens caused by linear absorption in GaAs limits the maximum achievable intracavity power. This is consistent with independent common-path interferometry measurements performed at $\lambda \approx 2 \mu\text{m}$ with epitaxially grown OP-GaAs that indicate residual absorption of $0.003\text{--}0.01 \text{ cm}^{-1}$ [14]. For example at 100 W of circulating power as much as 1 W may be dissipated inside the GaAs crystal.

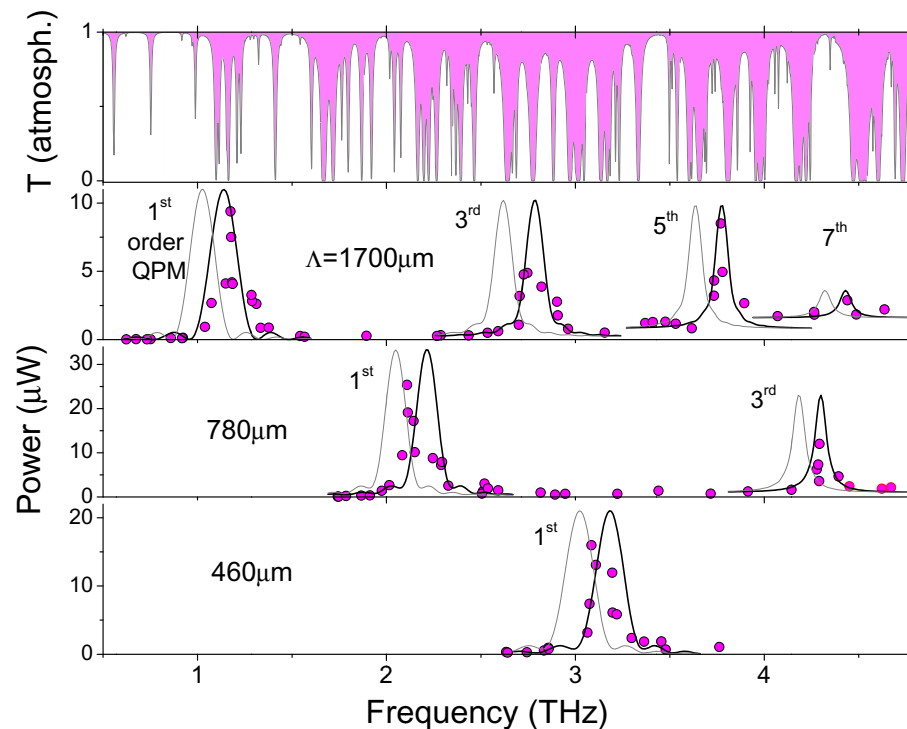
Although GaAs decreases the OPO performance in terms of maximum circulating intracavity power, our DR-OPO is perfectly suited to generate two waves with easily tunable difference frequencies across the whole THz range with a total optical power exceeding 100 W.

6. Generation of THz waves

To generate THz output via intracavity frequency mixing between the two closely spaced resonating OPO signal and idler waves, we have used three different OP-GaAs crystals (table 1). The OPO was pumped at 10 W, generating about 100 W of intracavity power near $2 \mu\text{m}$.

Table 1. OP-GaAs crystals used for intracavity THz generation and experimentally observed THz peaks.

| QPM period (μm) | Crystal length (mm) | First order QPM peak (THz) | Third order peak (THz) | Fifth order peak (THz) | Seventh order peak (THz) |
|------------------------------|---------------------|----------------------------|------------------------|------------------------|--------------------------|
| 1700 | 10 | 1.2 | 2.8 | 3.8 | 4.4 |
| 780 | 10 | 2.2 | 4.3 | – | – |
| 460 | 5 | 3.2 | – | – | – |

**Figure 4.** Emitted THz power versus frequency for three OP-GaAs samples with QPM periods of $\Lambda = 1700$, 780 and $460 \mu\text{m}$. Theoretical N th order quasi-phase matching curves (gray solid lines) were obtained from refractive index data of Stolen [19]. Black solid lines are theoretical curves obtained from the modified (see text) THz dispersion relations. Experimental data were distorted by THz absorption in the air: transmission of 25 cm of the atmosphere is shown on top.

By varying the temperature of the PPLN crystal, the difference frequency of the signal and idler fields was changed from 0.5 to 5 THz. Simultaneously, we measured the power of the THz wave extracted by the off-axis parabolic mirror and reaching the DLaTGS detector.

Figure 4 shows the results of THz tuning for the three OP-GaAs crystals. With the sample having $1700 \mu\text{m}$ QPM period, we observe as many as four phase matching peaks (bands) centered at approximately 1.2, 2.8, 3.8 and 4.4 THz with 9, 5, 8 and $1 \mu\text{W}$ output power, respectively. These bands correspond to the first, third, fifth and seventh order QPM processes [16]. At $780 \mu\text{m}$ QPM period, two phase matching bands are found at 2.2 and 4.3 THz

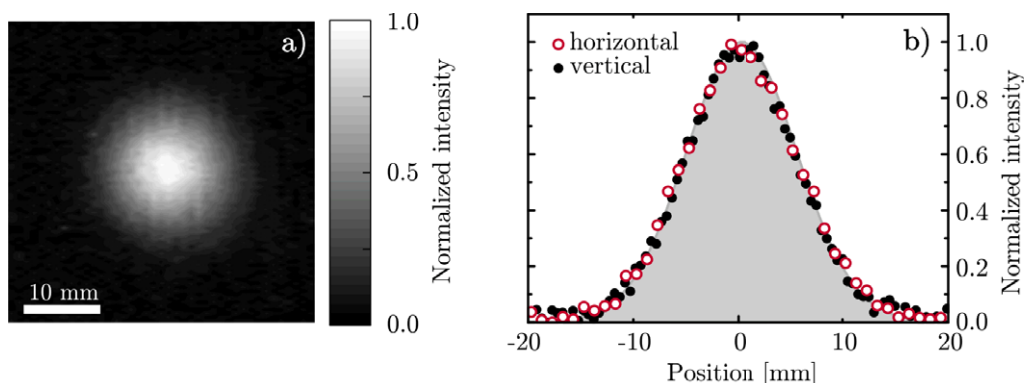


Figure 5. (a) Transversal normalized intensity distribution with (b) corresponding cross sections. The gray shaded area indicates a Gaussian distribution.

with 25.4 and 12 μW power, agreeing with the first and third order QPM, respectively. The 460 μm QPM period structure enables first order phase matching for the generation of a wave near 3.2 THz with 16 μW power. The shapes of the QPM peaks (as well as measured THz power) were strongly influenced by water vapor absorption in the atmosphere. Shown on top of figure 4 is the transmission of a 25 cm path of standard air taken from the HITRAN database (see footnote 6).

Theoretical N th order quasi-phase matching curves for difference frequency mixing in figure 4 were obtained using near-IR dispersion relations (measured specifically for OP-GaAs) from Skauli *et al* [17] and experimental GaAs THz refractive index data, which were best fitted to the functional form of Stolen *et al* [18], namely $n^2 = A + B/(1 - (\nu/\nu_0))^2$, where n is the refractive index, ν is the THz frequency, ν_0 is the GaAs phonon resonance frequency at 268.2 cm^{-1} (8.046 THz) and A and B are fitting parameters. The original THz dispersion relation from [17] ($A = 11.1$, $B = 1.95$, low-frequency $n = 3.61$) gives pretty large (~ 2 QPM bandwidths) deviation from our experimental data. On the other hand, THz refractive index data from Grischkowsky *et al* [19] (best fitted $A = 10.75$, $B = 2.138$, low-frequency $n = 3.59$) produced better fitting to our results (figure 4, gray curves). However our modified ($A = 10.58$, $B = 2.173$, low-frequency $n = 3.57$) dispersion relation produced a good match to all THz bands observed in our experiment (figure 4, black curves). The difference in THz refractive index data may arise on one hand from the fact that GaAs is grown by different methods (e.g. vapor phase epitaxy in our case versus melt growth in earlier works). On the other hand, the phase matching condition for focused beams (as in our case) is slightly different from that for plane waves. That may also explain deviation from tuning curves based on [19].

Additionally, we have determined the transversal intensity distribution of the emitted THz wave. The DLaTGS detector was covered with a metal plate having a 1 mm diameter hole transmitting a portion of THz light. We scanned this apparatus across the collimated THz beam at 2.1 THz frequency extracted by the off-axis parabolic mirror. Figures 5(a) and (b) show that the THz beam has a circular shape with an almost perfect Gaussian intensity distribution, thanks to the collinear phase matching scheme used here. This is opposite to the case of noncollinear intracavity difference frequency mixing inherently leads to an elliptic beam profile which has to be corrected by additional optical elements [11].

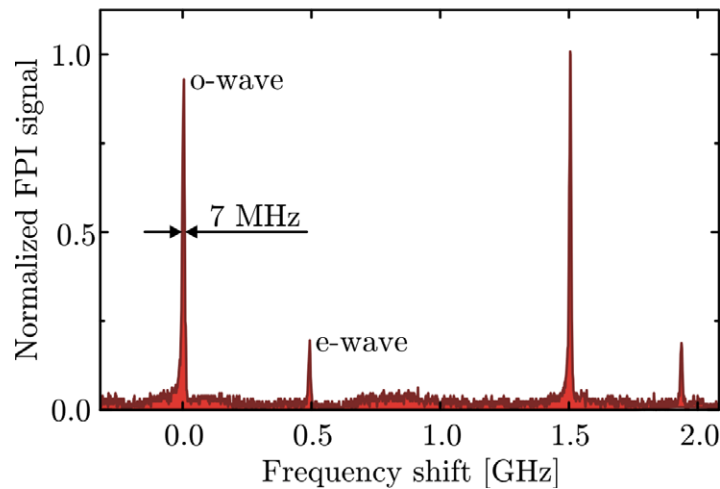


Figure 6. OPO signal (e-wave) and idler (o-wave) linewidths near $2\ \mu\text{m}$, measured with a scanning FPI (FSR = 1.5 GHz).

Thus, the system presented here emits CW THz light with a Gaussian beam profile and tunable from 1 to 4.5 THz with tens of μW power level. To emphasize the great potential of this source of monochromatic THz light, we take a closer look on the fifth order QPM process generating THz light at 3.8 THz with the $1700\ \mu\text{m}$ period GaAs structure. Here, the output power is about $8\ \mu\text{W}$. With a QPM period of $1700/5 = 340\ \mu\text{m}$, the effective nonlinear coefficient would increase by a factor of five [16]. This would increase the efficiency of the difference frequency generation by a factor of 25 and achieving $200\ \mu\text{W}$ of output power is straightforward. This value can be increased further. As shown in figure 2, the GaAs crystal decreases the intracavity power by a factor of 3 due to (i) absorption at the signal and idler wavelengths and (ii) induced thermal lens, which makes the resonator unstable. These effects can be reduced by using longer wavelength pump, e.g. in the $1.5\ \mu\text{m}$ telecom range, thus pushing the signal and idler wavelengths to $3\ \mu\text{m}$. In this case, we expect weaker residual absorption and consequently a higher intracavity power. At intracavity power level of $\sim 300\ \text{W}$ (demonstrated already with lithium niobate in the second focus), the output power of the THz light would grow by a factor of ~ 10 . Thus, monochromatic THz light tunable from 1 to 4.5 THz with powers in the milliwatt range should be achievable. Purging the setup (e.g. with nitrogen gas) will further increase the power performance of the presented system.

We have used three different OP-GaAs crystals in our experiment to cover piecewise the frequency range from 1 to 4.5 THz. For truly continuous tuning we will use a multi-grating OP-GaAs or an OP-GaAs with a fan-out grating. Both concepts were successfully implemented in PPLN and other QPM nonlinear crystals.

7. THz linewidth

The linewidths of the OPO signal and idler waves were measured using a scanning Fabry–Pérot Interferometer (FPI) with a free spectral range (FSR) of 1.5 GHz and finesse 200. The results of the measurements in two orthogonal polarizations are shown in figure 6. Since no neighboring modes are seen (the OPO mode spacing is $\sim 400\ \text{MHz}$), one can conclude that the OPO runs in a single longitudinal mode. The measured OPO linewidth (7 MHz) is the upper limit, since it is

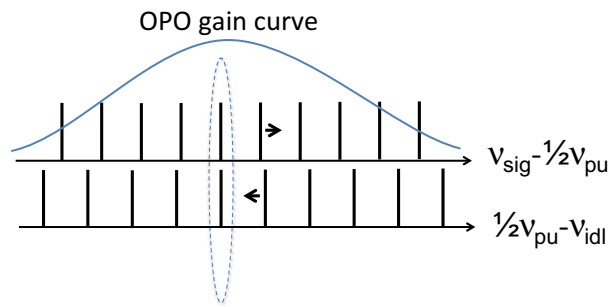


Figure 7. Mode-hop-free tuning of a DR-OPO. Vertical alignment of signal–idler pair in this coordinate system (signal grows to the right, idler to the left) ensures the conservation of the photon energy. Reducing the cavity length shifts the frequencies of the cavity modes in opposite directions (shown by arrows) and leads to hopping to the next signal–idler pair. Smooth tuning can be achieved by introducing a variable-thickness dispersive element in the cavity.

totally determined by the finesse of the FPI; the real linewidth can be much narrower. Thus we can conclude that the linewidth of the THz wave is definitely below 10 MHz.

It has been shown that a DR-OPO inherits the coherence of a pump laser and reproduces its linewidth. For instance, when a DR monolithic lithium niobate OPO was pumped by a narrow-linewidth (~ 10 kHz) laser, the OPO linewidth was equally narrow [20]. Furthermore, the linewidth of signal–idler heterodyne beat signal was measured to be even narrower: 500 Hz [20], the result of the fact that in the case of laser frequency variations, the latter are partially canceled because the signal and idler frequencies are subtracted from each other in a mixing process. Hence achieving kHz bandwidths of THz output in our system is feasible, provided that a narrow-linewidth pump laser is used.

8. Potential for continuous single-frequency THz tuning

Our DR-OPO approach allows achieving continuous single-frequency THz tuning via mode-hop-free tuning of the OPO signal and idler waves, which is illustrated in figure 7. The DR-OPO is inherently a single-frequency device, because of the constraints imposed by the requirement of resonating simultaneously at signal and idler frequencies [21], and also due to the fact that signal and idler have in general different mode spacing (e.g. as a result of chromatic dispersion and birefringence of lithium niobate). If one changes the cavity length, the signal and idler frequencies in general will hop. To prevent this and to achieve smooth tuning, one can insert a dispersive element in the form of a wedge inside the ring OPO cavity, such that the tuning can be performed continuously over long spectral regions with no breaks or mode hops by a combined tuning of cavity length and wedge thickness.

9. Conclusion

In summary, we described a novel OP-GaAs based source for producing high power ($> 10 \mu\text{W}$) diffraction limited and narrow linewidth THz waves tunable over the range between 1 and 4.5 THz, scalable to milliwatts. Due to its narrow linewidth, high spectral brightness and excellent beam quality, this source can be crucial for numerous nonlinear THz studies including Doppler-free saturation spectroscopy, multicolor (THz plus mid-IR) spectroscopy, coherent control and quantum path engineering.

Acknowledgments

KLV thanks NASA and the Office of Naval Research for financial support. The authors gratefully acknowledge support by the German Research Foundation (DFG), BU 913/21.

References

- [1] Siegel P H 2002 Terahertz technology *IEEE Trans. Microw. Theory Tech.* **50** 910–28
- [2] Mittleman D 2003 *Sensing with Terahertz Radiation* (Berlin: Springer) pp 39–115
- [3] Yeh K L, Hoffmann M C, Hebling J and Nelson K A 2007 Generation of 10 μ J ultrashort terahertz pulses by optical rectification *Appl. Phys. Lett.* **90** 171121
- [4] Demtröder W 2008 *Laser Spectroscopy: Experimental Techniques* vol 2, 4th edn (Dordrecht: Springer) pp 77–140
- [5] Winnewisser G, Belov S P, Klaus Th and Schieder R 1997 Sub-Doppler measurements on the rotational transitions of carbon monoxide *J. Mol. Spectrosc.* **184** 468–72
- [6] Brown E R, McIntosh K A, Nichols K B and Dennis C L 1995 Photomixing up to 3.8 THz in low-temperature-grown GaAs *Appl. Phys. Lett.* **66** 285–7
- [7] Verghese S, McIntosh K A and Brown E R 1997 Highly tunable fiber coupled photomixers with coherent terahertz output power *IEEE Trans. Microw. Theory Tech.* **45** 1301–9
- [8] Staus C, Kuech T and McCaughan L 2008 Continuously phase-matched terahertz difference frequency generation in an embedded waveguide structure supporting only fundamental modes *Opt. Express* **16** 13296–303
- [9] Sowade R, Breunig I, Camara Mayorga I, Kiessling J, Tulea C, Dierolf V and Buse K 2009 Continuous-wave optical parametric terahertz source *Opt. Express* **17** 22303–10
- [10] Kiessling J, Fuchs F, Buse K and Breunig I 2011 Pump-enhanced optical parametric oscillator generating continuous wave tunable terahertz radiation *Opt. Lett.* **36** 4374–6
- [11] Scheller M, Yarborough J M, Moloney J V, Fallahi M, Koch M and Koch S W 2010 Room temperature continuous wave milliwatt terahertz source *Opt. Express* **18** 27112–17
- [12] Schaar J E, Vodopyanov K L and Fejer M M 2007 Intracavity terahertz-wave generation in a synchronously pumped optical parametric oscillator using quasi-phase-matched GaAs *Opt. Lett.* **32** 1284–6
- [13] Eyres L A, Turreau P J, Pinguet T J, Ebert C B, Harris J S, Fejer M M, Becouarn L, Gerard B and Lallier E 2001 All-epitaxial fabrication of thick, orientation-patterned GaAs films for nonlinear optical frequency conversion *Appl. Phys. Lett.* **79** 904–6
- [14] Markosyan A 2013 private communications, Ginzton Laboratory, Stanford University
- [15] Mansell J D, Hennawi J, Gustafson E K, Fejer M M, Byer R L, Clubley D, Yoshida S and Reitze D H 2001 Evaluating the effect of transmissive optic thermal lensing on laser beam quality with a Shack–Hartmann wave-front sensor *Appl. Optics* **40** 366–74
- [16] Vodopyanov K L 2008 *Laser Photon. Rev.* **2** 11–25
- [17] Skauli T *et al* 2003 Improved dispersion relations for GaAs and applications to nonlinear optics *J. Appl. Phys.* **94** 6447–55
- [18] Stolen R H 1969 Far infrared absorption in high resistivity GaAs *Appl. Phys. Lett.* **15** 74–5
- [19] Grischkowsky D, Keiding S, van Exter M and Fattinger Ch 1990 Far-infrared time-domain spectroscopy with terahertz beams of dielectrics and semiconductors *J. Opt. Soc. Am. B* **7** 2006–15
- [20] Nabors C D, Yang S T, Day T and Byer R L 1990 Coherence properties of a doubly-resonant monolithic optical parametric oscillator *J. Opt. Soc. Am. B* **7** 815–20
- [21] Scherrer B, Ribet I, Godard A, Rosencher E and Lefebvre M 2000 Dual-cavity doubly resonant optical parametric oscillators, demonstration of pulsed single-mode operation *J. Opt. Soc. Am. B* **17** 1716–29